

Supporting Material

Hydrogenation of CO₂ on nanostructured Cu/FeO_x catalysts: The effect of morphology and Cu load on selectivity

Karolína Simkovičová^{1,2}, Muhammad I. Qadir¹, Naděžda Žilková¹, Joanna E. Olszówka¹, Pavel Sialini³, Libor Kvítek^{2*} and Štefan Vajda^{1*}

¹ Department of Nanocatalysis, J. Heyrovský Institute of Physical Chemistry v.v.i., Czech Academy of Sciences, Dolejškova 2155/3, 182 23 Prague 8, Czech Republic.

² Department of Physical Chemistry, Faculty of Science, Palacký University Olomouc, 17. listopadu 12, 77900 Olomouc, Czech Republic.

³ Laboratory of Surface Analysis, University of Chemistry and Technology, Technická 3, 16628 Prague, Czech Republic.

* Correspondence: stefan.vajda@jh-inst.cas.cz (SV) and libor.kvitek@upol.cz (LK)

Table of content:

| | | |
|------------|---|-----|
| Figure S1 | Temperature ramp..... | S2 |
| Figure S2 | SEM/EDX of fresh catalysts | S3 |
| Figure S3 | STEM/HAADF images of fresh FeO _x | S4 |
| Figure S4 | STEM/HAADF images of fresh 1%-Cu/FeO _x | S5 |
| Figure S5 | STEM/HAADF images of fresh 3%-Cu/FeO _x | S6 |
| Figure S6 | STEM/HAADF images of fresh 5%-Cu/FeO _x | S7 |
| Figure S7 | XRD patterns of fresh catalysts | S8 |
| Table S1 | X-ray coherence length of fresh catalysts..... | S9 |
| Figure S8 | XPS of fresh and spent catalysts..... | S10 |
| Figure S9 | XPS of FeO _x | S11 |
| Table S2 | Chemical composition of Fe and Cu in catalysts | S11 |
| Figure S10 | Wide scan XPS spectra of fresh and spent catalysts | S12 |
| Figure S11 | Adsorption/desorption isotherms of fresh catalysts | S13 |
| Figure S12 | UV-Vis spectra of fresh catalysts..... | S14 |
| Table S3 | Conversion and selectivities of FeO _x , 1%-Cu/FeO _x , 3%-Cu/FeO _x and 5%-Cu/FeO _x | S15 |
| Figure S13 | TEM images of fresh and spent catalysts..... | S16 |
| Figure S14 | SEM/EDX of spent catalysts..... | S17 |
| Figure S15 | STEM/HAADF images of spent FeO _x | S18 |
| Figure S16 | STEM/HAADF images of spent 1%-Cu/FeO _x | S19 |
| Figure S17 | STEM/HAADF images of spent 3%-Cu/FeO _x | S20 |
| Figure S18 | XRD patterns of spent catalysts | S21 |
| Table S4 | Mean X-ray coherence length of spent catalysts..... | S22 |
| Figure S19 | Adsorption/desorption isotherms of spent catalysts | S23 |
| Figure S20 | Comparison of the performance of the catalysts | S24 |
| Figure S21 | CO ₂ conversion and selectivity over the course of 6 consecutive temperature ramps | S25 |
| Table S5 | Literature comparison of CO ₂ hydrogenation by different iron-based catalysts | S26 |
| Figure S22 | Literature comparison of CO ₂ hydrogenation by different iron-based catalysts | S27 |
| | References | S28 |

Temperature ramp

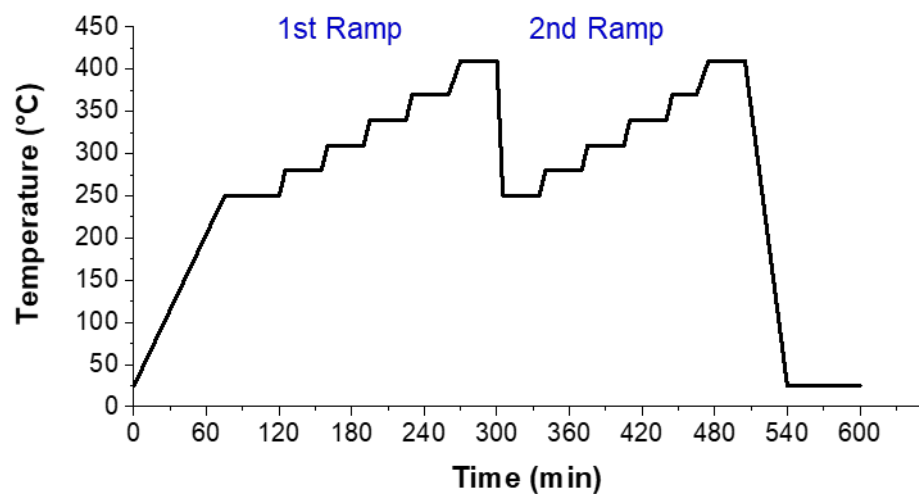


Figure S1. Double temperature ramp applied during catalytic testing. 200 mg of catalyst and CO₂/H₂/He (1:5:4, total flow 25 ml/min).

SEM/EDX of fresh catalysts

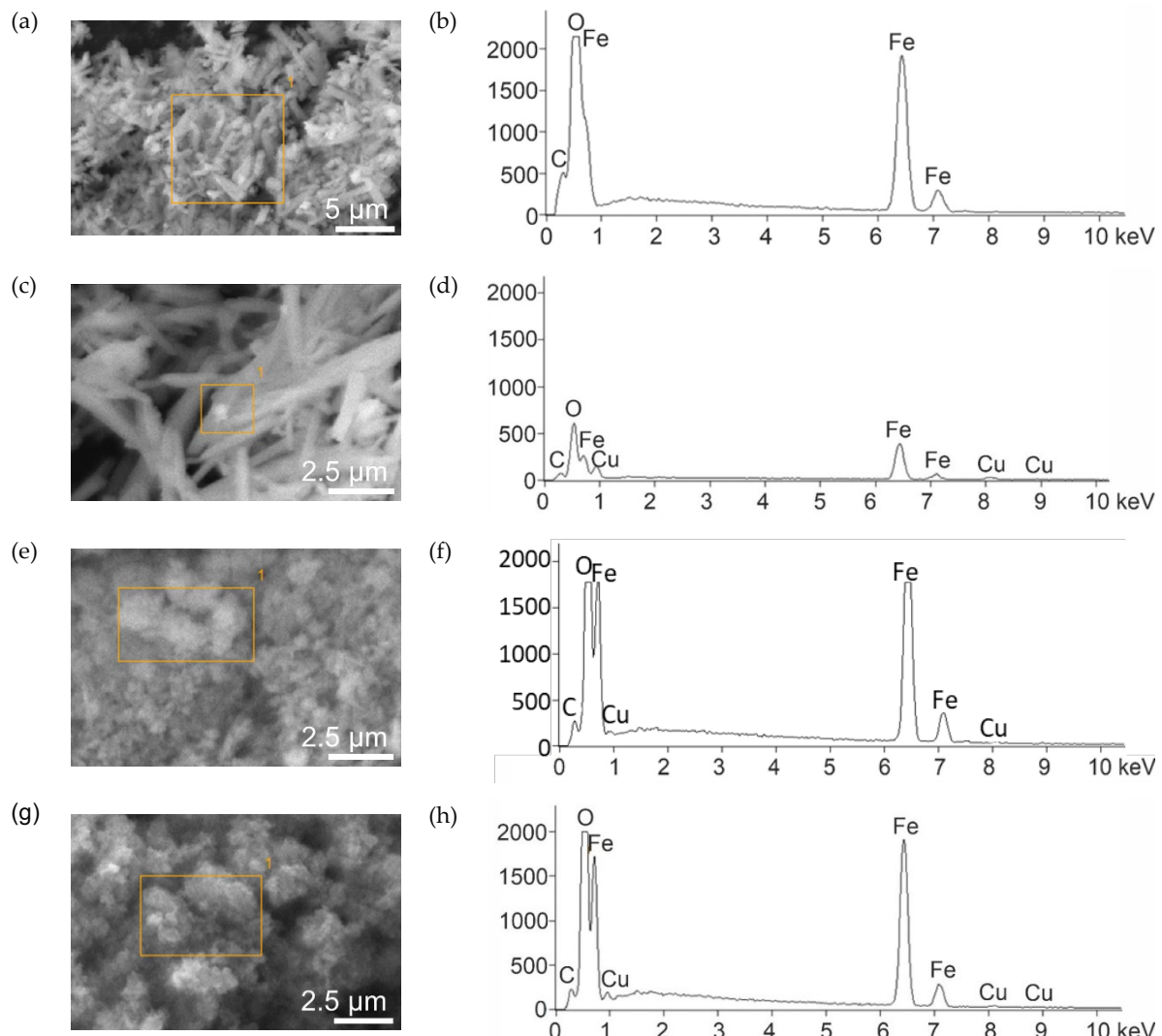


Figure S2. SEM images of fresh catalysts and EDX of the selected part of the image in highlighted rectangles with included particles, (a, b) FeO_x, (c, d) 1%-Cu/FeO_x, (e, f) 3%-Cu/FeO_x and (g, h) 5%-Cu/FeO_x.

STEM/HAADF images of fresh FeO_x

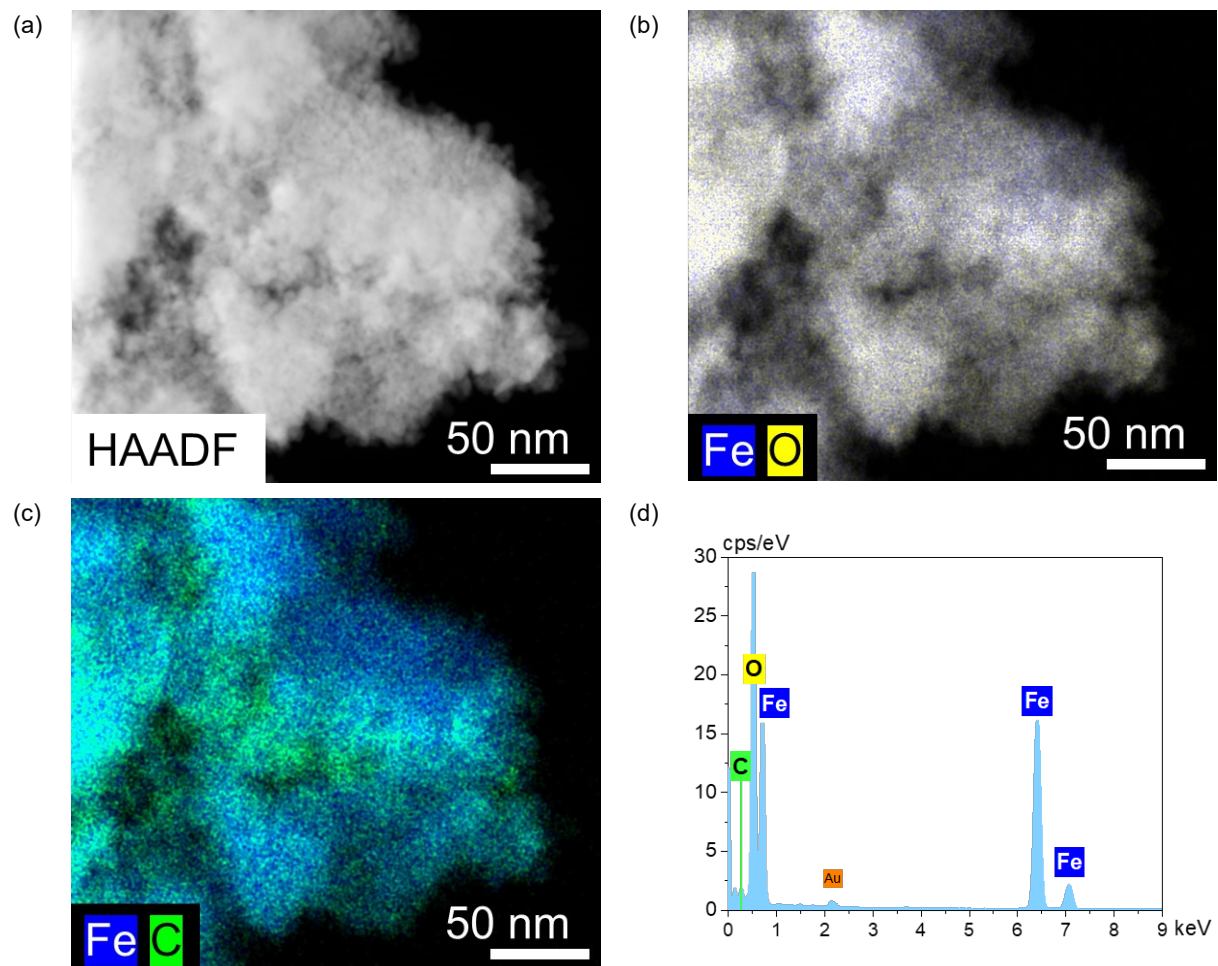


Figure S3. (a) STEM-HAADF of fresh FeO_x, and (b-d) EDX elemental mapping (red: Fe, yellow: O, green: C)

STEM/HAADF images of fresh 1%-Cu/FeO_x

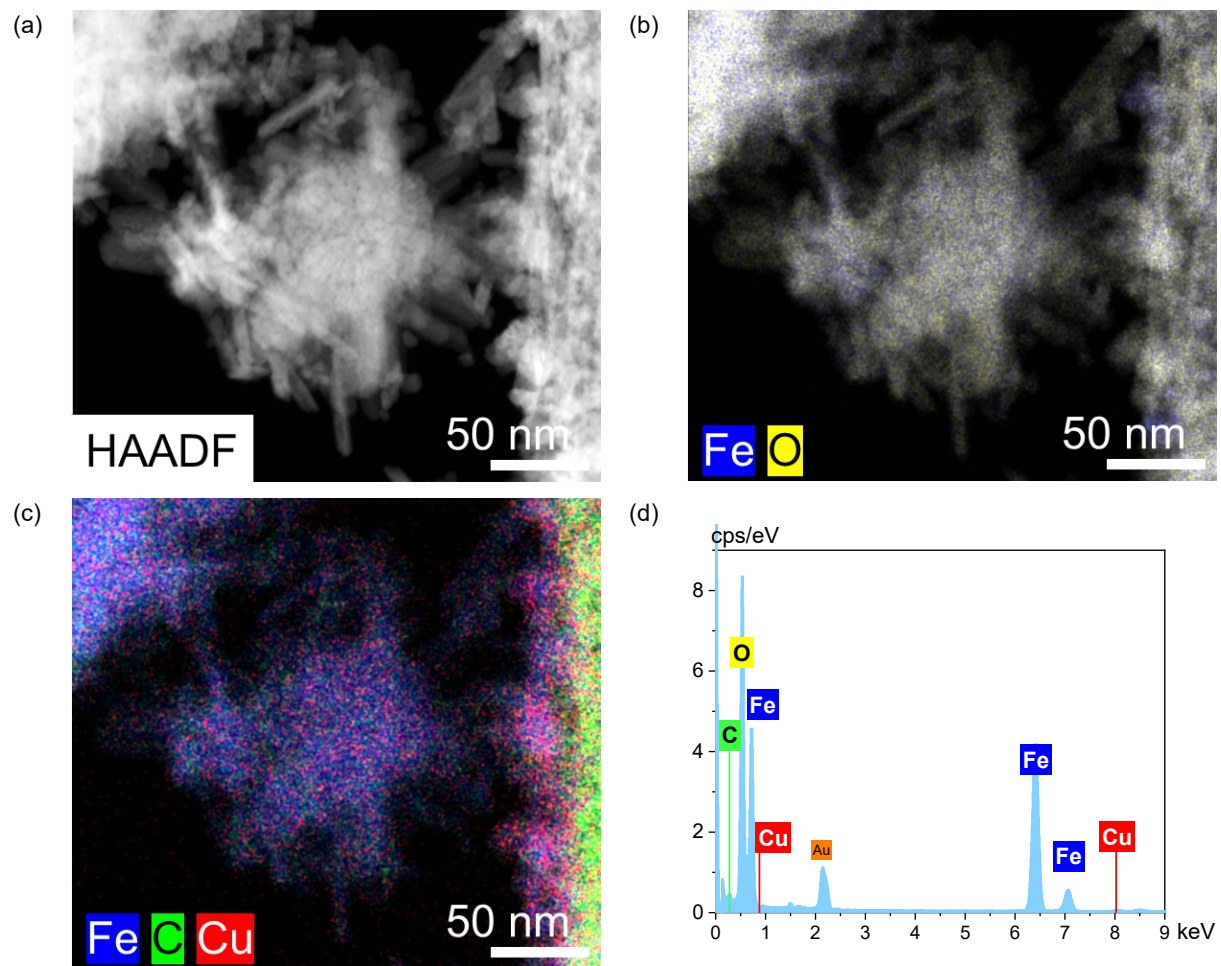


Figure S4. (a) STEM-HAADF of fresh 1%-Cu/FeO_x, and (b-d) EDX elemental mapping of Fe, O, C and Cu.

STEM/HAADF images of fresh 3%-Cu/FeO_x

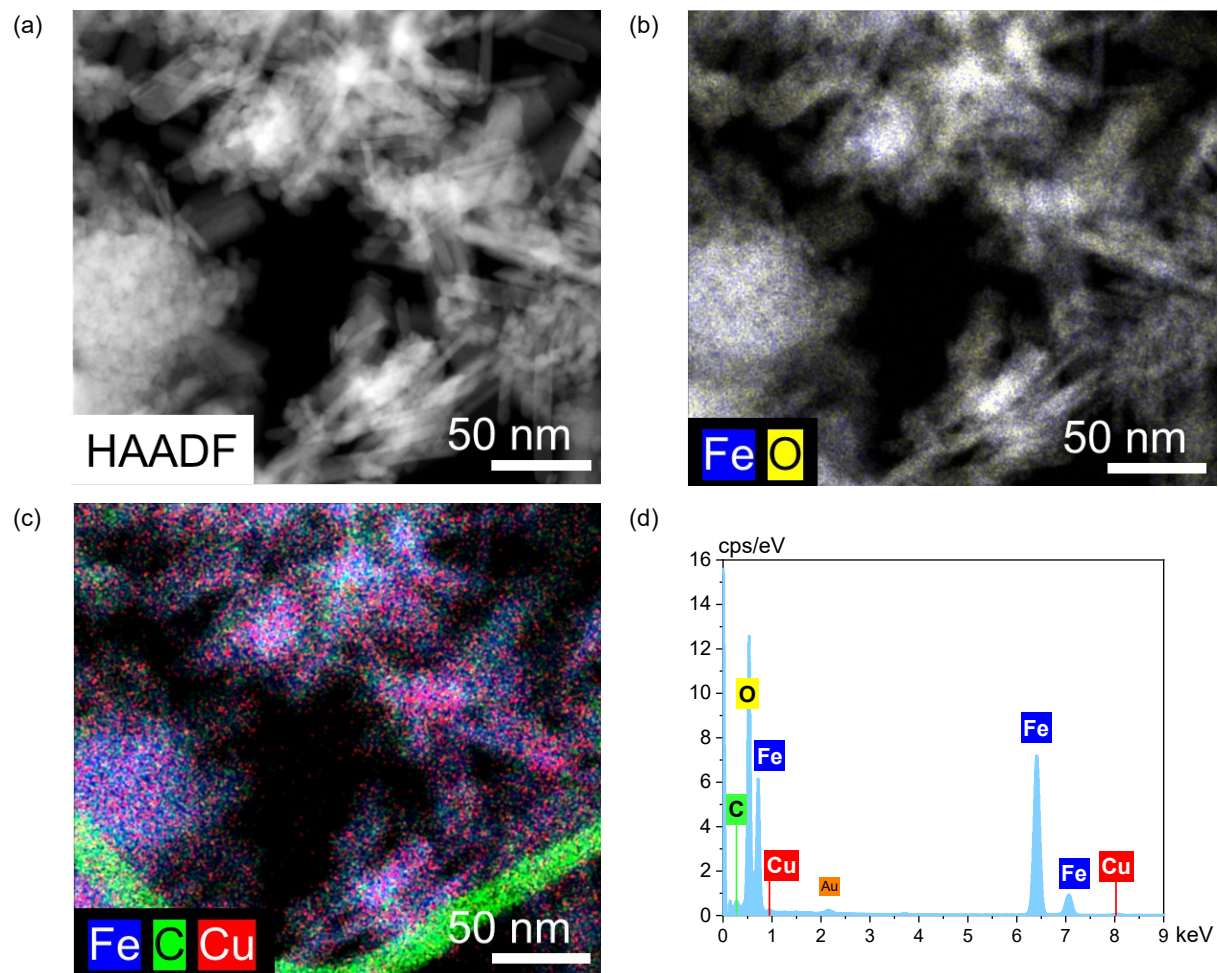


Figure S5. (a) STEM-HAADF of fresh 3%-Cu/FeO_x, and (b-d) EDX elemental mapping of Fe, O, C and Cu.

STEM/HAADF images of fresh 5%-Cu/FeO_x

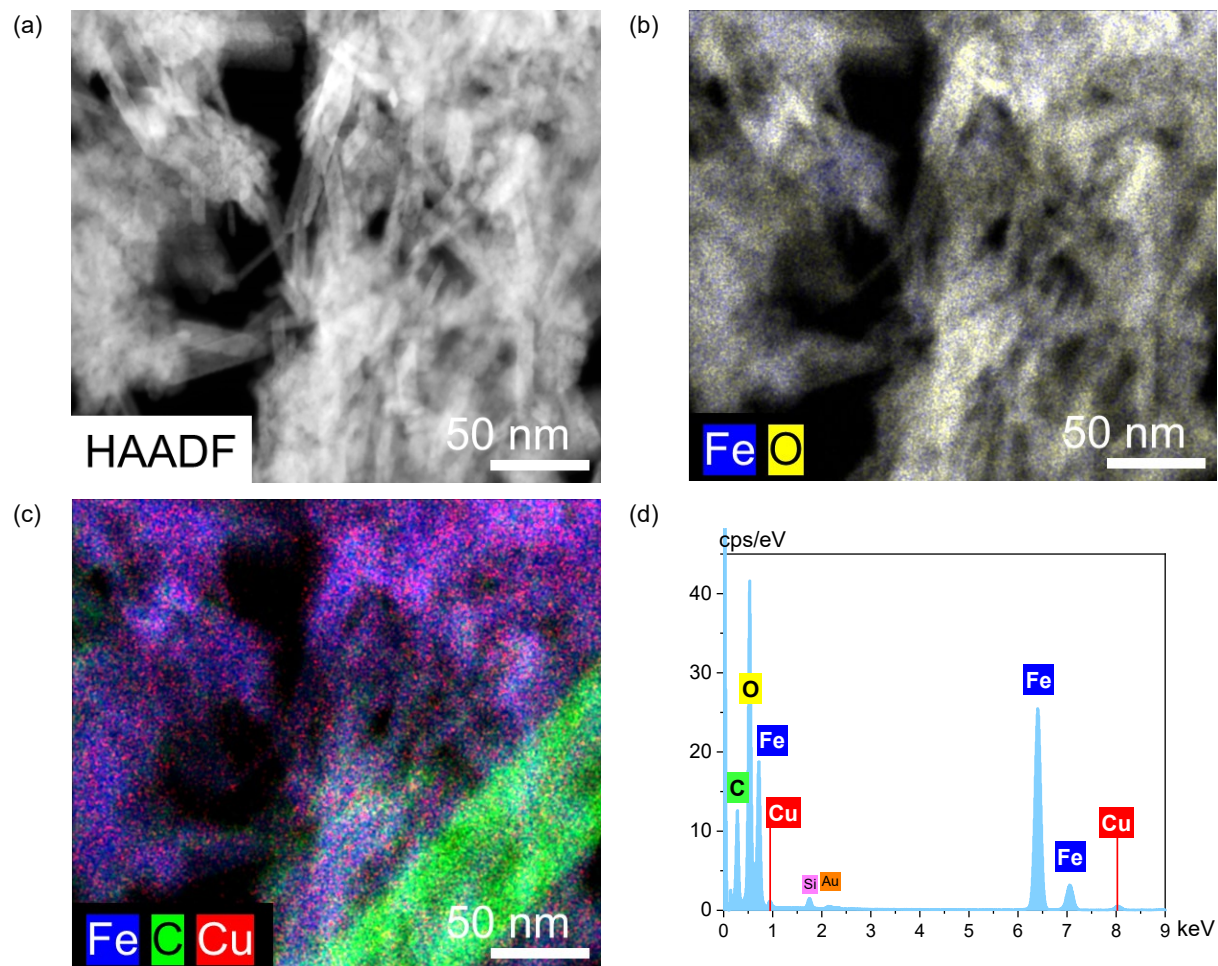


Figure S6 (a) STEM-HAADF of fresh 5%-Cu/FeO_x, and (b-d) EDX elemental mapping of Fe, O, C and Cu.

XRD patterns of fresh catalysts

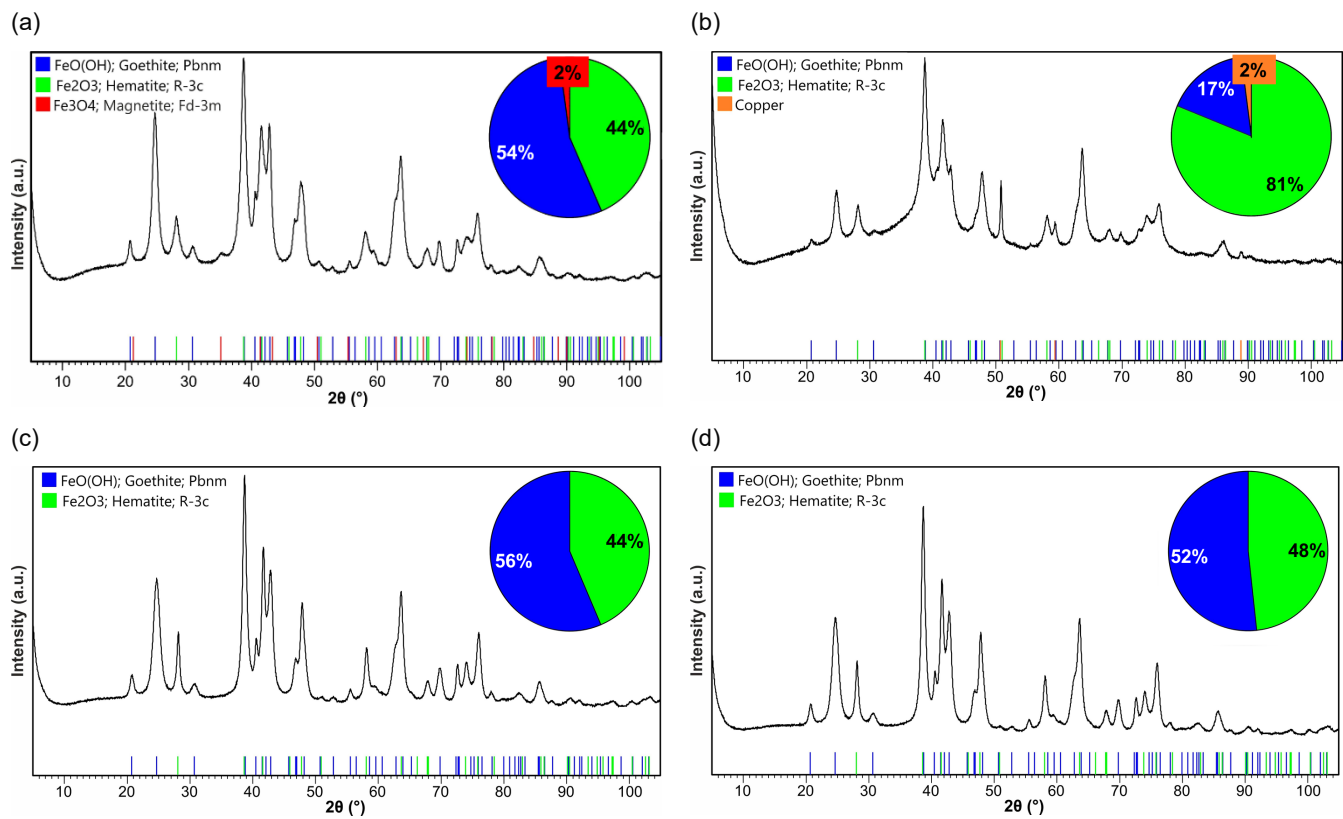


Figure S7. XRD patterns of fresh (a) FeO_x, (b) 1%-Cu/FeO_x, (c) 3%-Cu/FeO_x and (d) 5%-Cu/FeO_x.

Mean X-ray coherence length of fresh catalysts

Table S1. Mean X-ray coherence length of fresh catalysts obtained from XRD data using Rietveld refinement of analysis.

| Catalyst | $\alpha\text{-Fe}_2\text{O}_3$ [nm] | $\alpha\text{-FeO(OH)}$ [nm] | Fe_3O_4 [nm] |
|------------------------|--|---------------------------------|---------------------------------|
| FeO _x | 9 | 12 | 11 |
| 1%-Cu/FeO _x | 12 | 11 | 0.0 |
| 3%-Cu/FeO _x | 19 | 9 | 0.0 |
| 5%-Cu/FeO _x | 19 | 10 | 0.0 |

XPS of fresh and spent catalysts

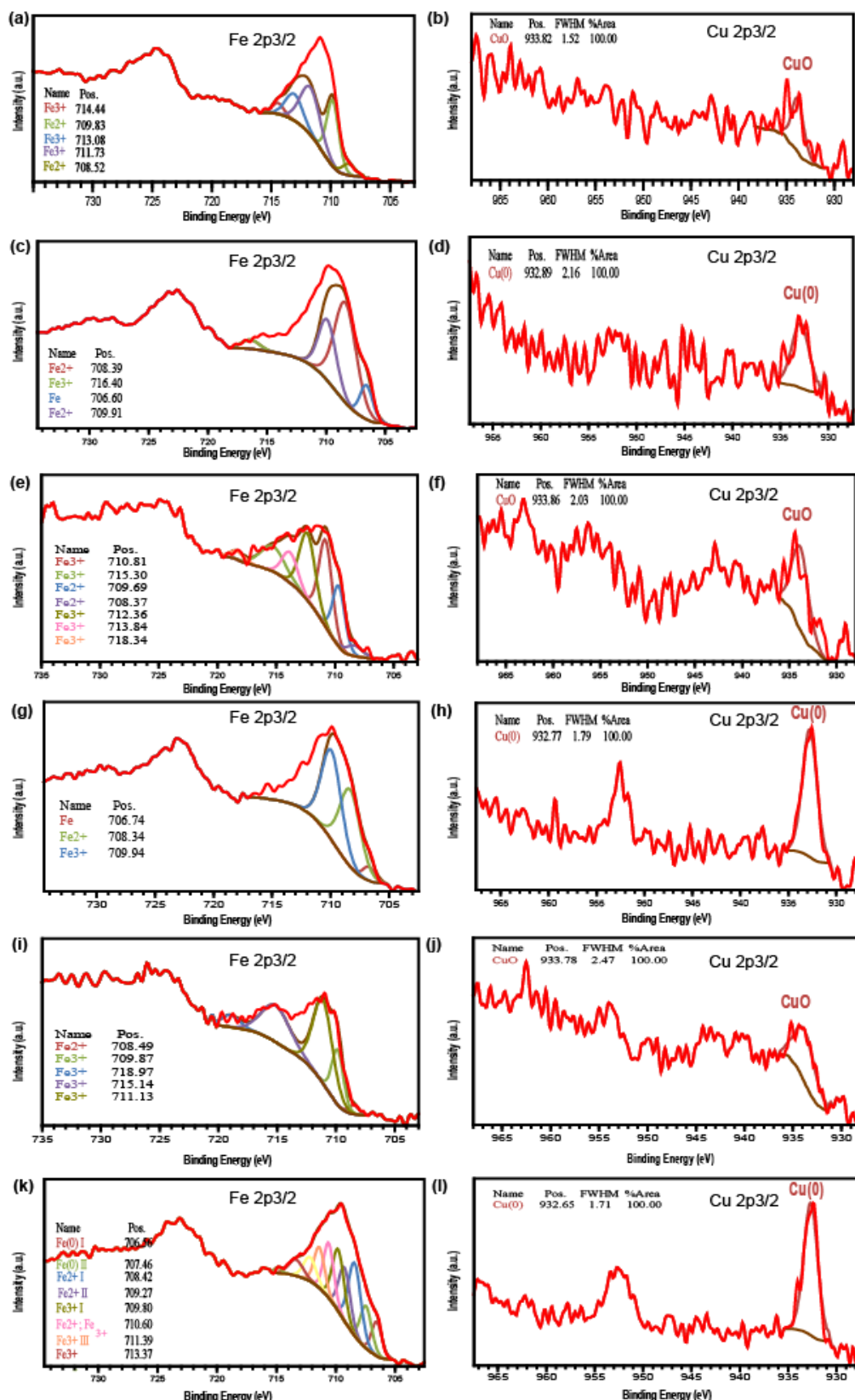


Figure S8. XPS analysis; quantification and deconvoluted spectra of copper and iron for catalysts (a, b) fresh 1%-Cu/FeO_x, (c, d) spent 1%-Cu/FeO_x, (e, f) fresh 3%-Cu/FeO_x, (g, h) spent 3%-Cu/FeO_x, (i, j) fresh 5%-Cu/FeO_x, and (k, l) spent 5%-Cu/FeO_x

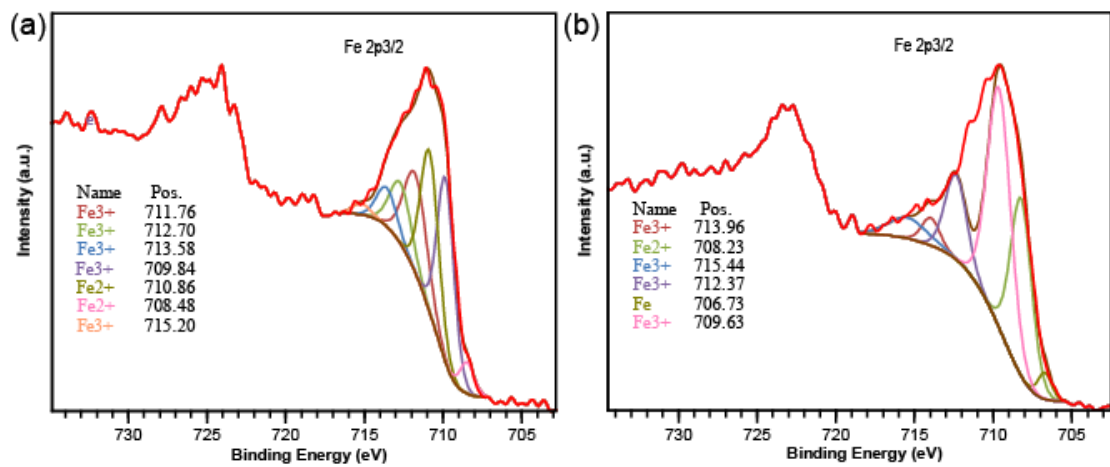


Figure S9. XPS analysis; quantification and deconvoluted spectra iron for catalysts (a) fresh FeO_x , and (b) spent FeO_x .

Table S2. Chemical composition of Fe and Cu in catalysts.

| Catalyst | Fe(0) | Fe ²⁺ | Fe ³⁺ | Cu ²⁺ | Cu(0) |
|----------------------------|-------|------------------|------------------|------------------|-------|
| Fresh 1%Cu/ FeO_x | - | + | + | + | - |
| Spent 1%Cu/ FeO_x | + | + | + | - | + |
| Fresh 3%Cu/ FeO_x | - | + | + | + | - |
| Spent 3%Cu/ FeO_x | + | + | + | - | + |
| Fresh 5%Cu/ FeO_x | - | + | + | + | - |
| Spent 5%Cu/ FeO_x | + | + | + | - | + |
| Fresh FeO_x | - | + | + | - | - |
| Spent FeO_x | + | + | + | - | - |

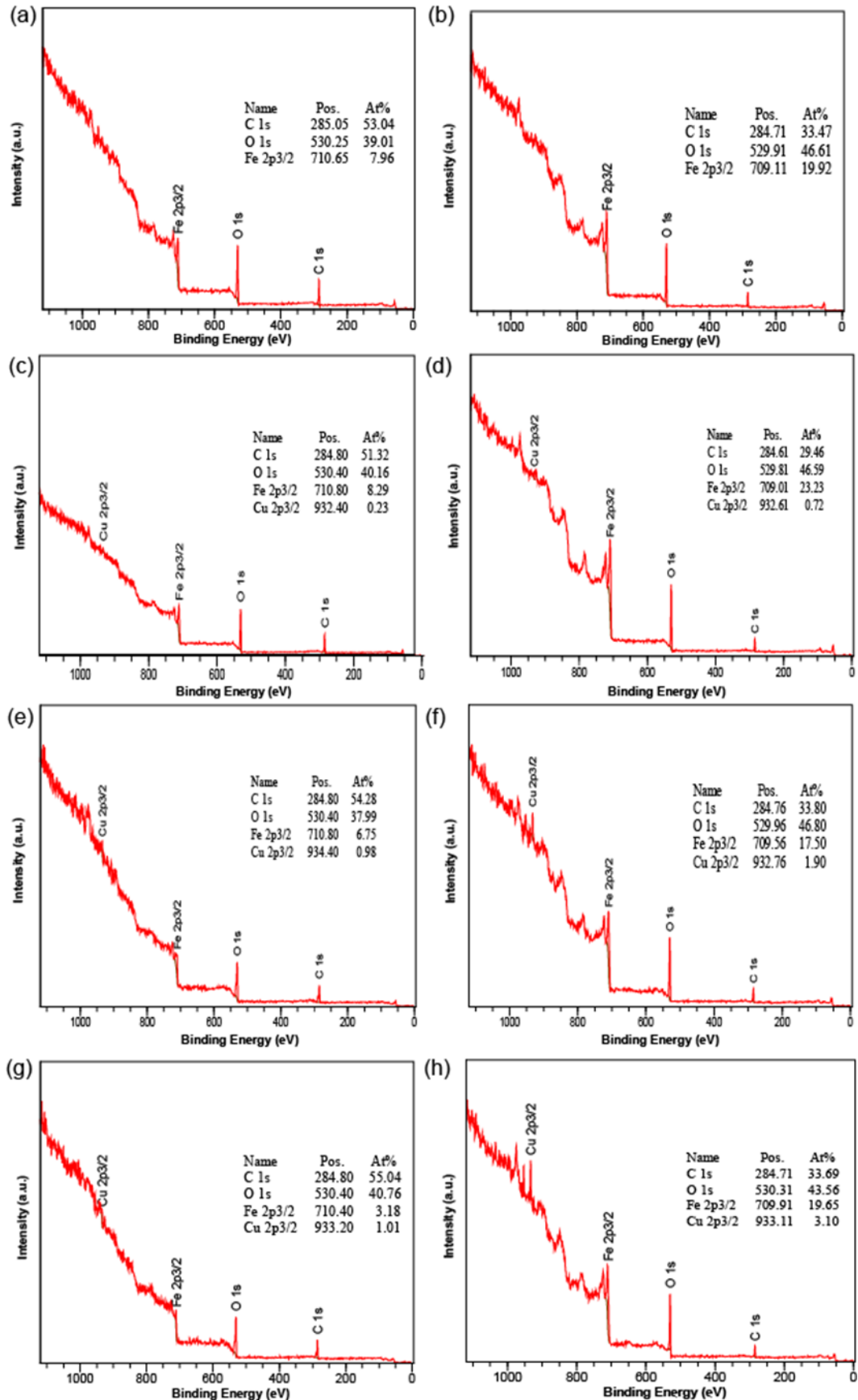


Figure S10. Wide scan XPS spectra of (a, b) fresh and spent FeO_x , (c, d) fresh and spent 1% Cu/ FeO_x , (e, f) fresh and spent 3% Cu/ FeO_x , (g, h) fresh and spent 5% Cu/ FeO_x , respectively.

Adsorption/desorption isotherms of fresh catalysts

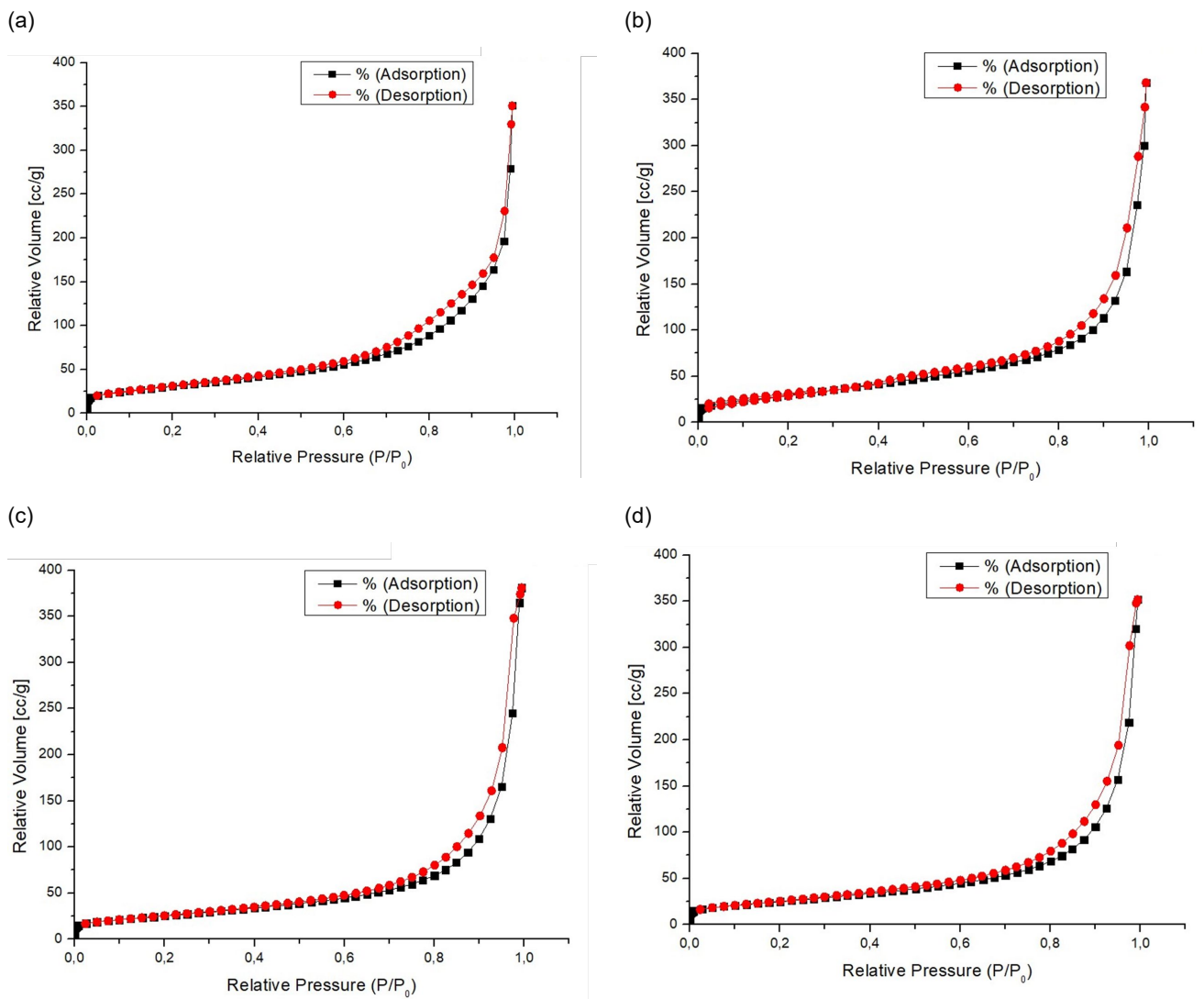


Figure S11. Adsorption and desorption isotherms of fresh (a) blank FeO_x , (b) 1%-Cu/ FeO_x , (c) 3%-Cu/ FeO_x and (d) 5%-Cu/ FeO_x .

UV-Vis spectra of fresh catalysts

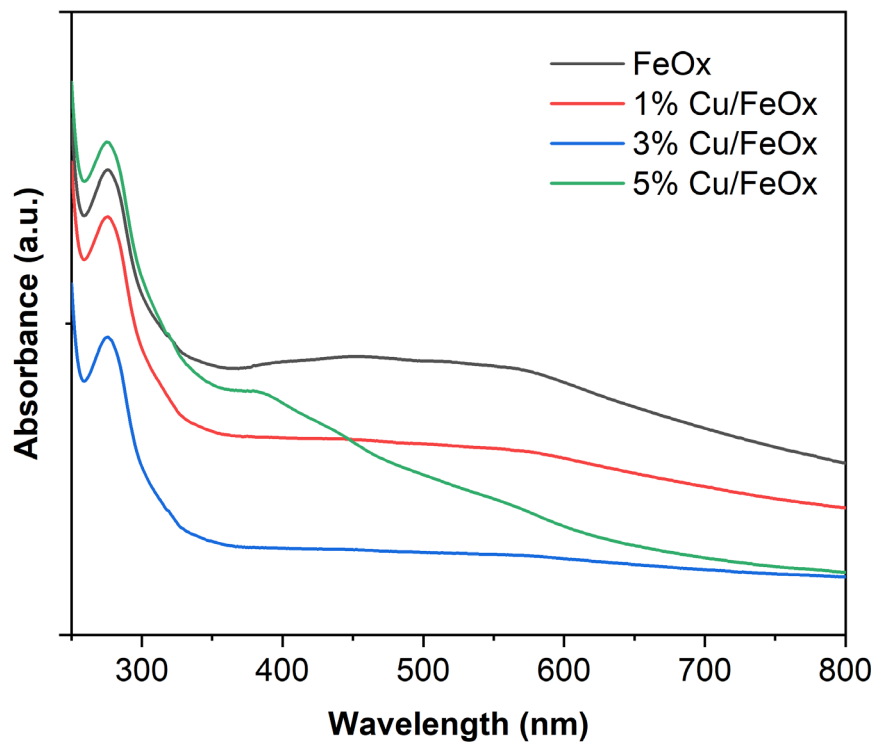


Figure S12. UV-Vis spectra of fresh catalysts. The spectra were recorded in glycerol.

Conversion and selectivities of FeO_x, 1%-Cu/FeO_x, 3%-Cu/FeO_x and 5%-Cu/FeO_x

Table S3: CO₂ conversion and product selectivities during 1st and 2nd temperature ramps. Reaction mixture was CO₂, H₂ and He in the ratio of 1:5:4 giving 11 % and 49 % of CO₂ and H₂ in He, respectively. Total flow 25 mL/min, pressure 1 bar. Products were analysed by gas chromatography.

| Cat. | T [°C] | CO ₂ conversion [%] | | Selectivity [%] | | | | | | | | | | |
|------------------------|--------|--------------------------------|------|-----------------|------|--------------------------------|------|----------------------------------|------|-----------------|------|-----|----|------|
| | | | | CH ₄ | | C ₂ -C ₄ | | C ₂ -C ₄ = | | C ₅₊ | | CO | | |
| ramp | 1. | 2. | 1. | 2. | 1. | 2. | 1. | 2. | 1. | 2. | 1. | 2. | 1. | 2. |
| FeO _x | 250 | 1.5 | - | 100 | 100 | - | - | - | - | - | - | - | - | - |
| | 280 | 2 | 0.7 | 100 | 100 | - | - | - | - | - | - | - | - | - |
| | 310 | 3.1 | 2.4 | 90.9 | 81.5 | - | - | 9.1 | 6.2 | - | - | - | - | 12.3 |
| | 340 | 7.9 | 6.9 | 26.2 | 71.2 | 18 | - | 36.4 | 14.4 | 19.5 | - | - | - | 14.5 |
| | 370 | 14.9 | 14 | 19.2 | 57.6 | 22.7 | - | 31.9 | 10.5 | 26.2 | - | - | - | 31.9 |
| | 410 | 30.3 | 28.2 | 29.7 | 80 | 25 | - | 31.6 | 20 | 13.7 | - | - | - | - |
| 1%-Cu/FeO _x | 250 | - | 1.4 | - | 69.5 | - | 22.8 | - | 6.1 | - | - | - | - | 1.6 |
| | 280 | - | 3.4 | 100 | 69.1 | - | 17.9 | - | 10.1 | - | 1.25 | - | - | 1.6 |
| | 310 | 3.5 | 8.3 | 39.5 | 66.5 | 12 | 13.1 | 45 | 16.1 | 3.4 | 2.2 | - | - | 2.1 |
| | 340 | 14.7 | 13 | 50.1 | 65.4 | 13.6 | 8.5 | 27 | 21.8 | 6.6 | 2 | 2.7 | - | 2.4 |
| | 370 | 23.5 | 21.6 | 60.5 | 64.5 | 5.7 | 5.8 | 29 | 25.6 | 2.3 | 1.5 | 2.5 | - | 2.7 |
| | 410 | 34.7 | 34.4 | 73.3 | 75.2 | 3.4 | 4.3 | 19.9 | 17.4 | 0.5 | 0.4 | 3 | - | 2.7 |
| 3%-Cu/FeO _x | 250 | 2.3 | 7.3 | 96 | 62.2 | - | 32.3 | - | - | - | 2.8 | 4 | - | 2.8 |
| | 280 | 6.2 | 10.9 | 83.5 | 58.5 | 5.2 | 34.2 | 8.3 | 2.2 | - | 2.4 | 3.3 | - | 2.6 |
| | 310 | 13 | 17.3 | 67.7 | 56.7 | 11.4 | 31.7 | 17.2 | 5.6 | 1.3 | 3.5 | 2.8 | - | 2.5 |
| | 340 | 19.1 | 22.9 | 60.9 | 59.6 | 15.1 | 24.2 | 18 | 10.9 | 3.5 | 2.8 | 2.5 | - | 2.6 |
| | 370 | 27.3 | 26.8 | 62.7 | 66.3 | 17.7 | 14.2 | 14.6 | 15.1 | 2.3 | 1.4 | 2.7 | - | 3.1 |
| | 410 | 36.5 | 36.8 | 82.6 | 82.2 | 6.5 | 6.2 | 6.9 | 8 | 0.4 | - | 3.6 | - | 3.6 |
| 5%-Cu/FeO _x | 250 | 1.4 | 5.6 | 100 | 57 | - | 37.3 | - | 0.3 | - | 2.9 | - | - | 2.6 |
| | 280 | 5.6 | 11.8 | 78.4 | 55.3 | 8 | 36.4 | 7.1 | 1.8 | - | 3.9 | 6.5 | - | 2.5 |
| | 310 | 12 | 17 | 69.3 | 54.3 | 17.7 | 34.8 | 9 | 3.5 | 1.3 | 4 | 2.7 | - | 3.3 |
| | 340 | 20 | 23.7 | 66.9 | 57.6 | 20.4 | 29.7 | 6.8 | 6.4 | 1.9 | 3 | 4.1 | - | 3.3 |
| | 370 | 27.8 | 29.5 | 78.3 | 68.6 | 12.3 | 18.6 | 4.5 | 7.2 | 0.4 | 1.3 | 4.4 | - | 4.3 |
| | 410 | 35 | 35.6 | 92.3 | 86.6 | 2.4 | 4 | 0.2 | 2.7 | - | 1.3 | 5.1 | - | 5.4 |

TEM images of fresh and spent catalysts

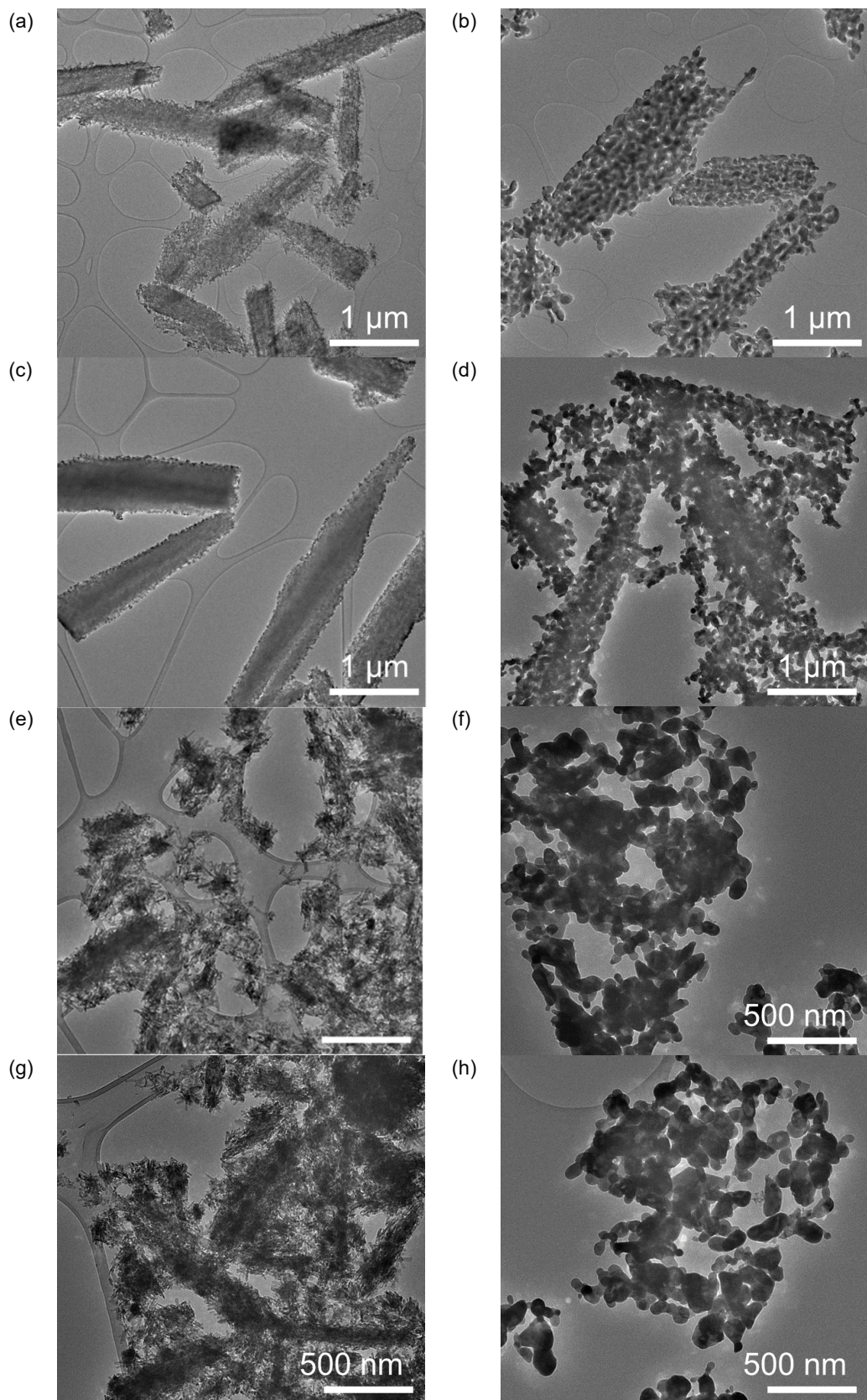


Figure S13: TEM images of (a) fresh FeO_x and (b) spent FeO_x , (c) fresh 1%-Cu/ FeO_x and (d) spent 1%-Cu/ FeO_x , (e) fresh 3%-Cu/ FeO_x and (f) spent 3%-Cu/ FeO_x , (g) fresh 5%-Cu/ FeO_x and (h) spent 5%-Cu/ FeO_x catalyst.

SEM/EDX of spent catalysts

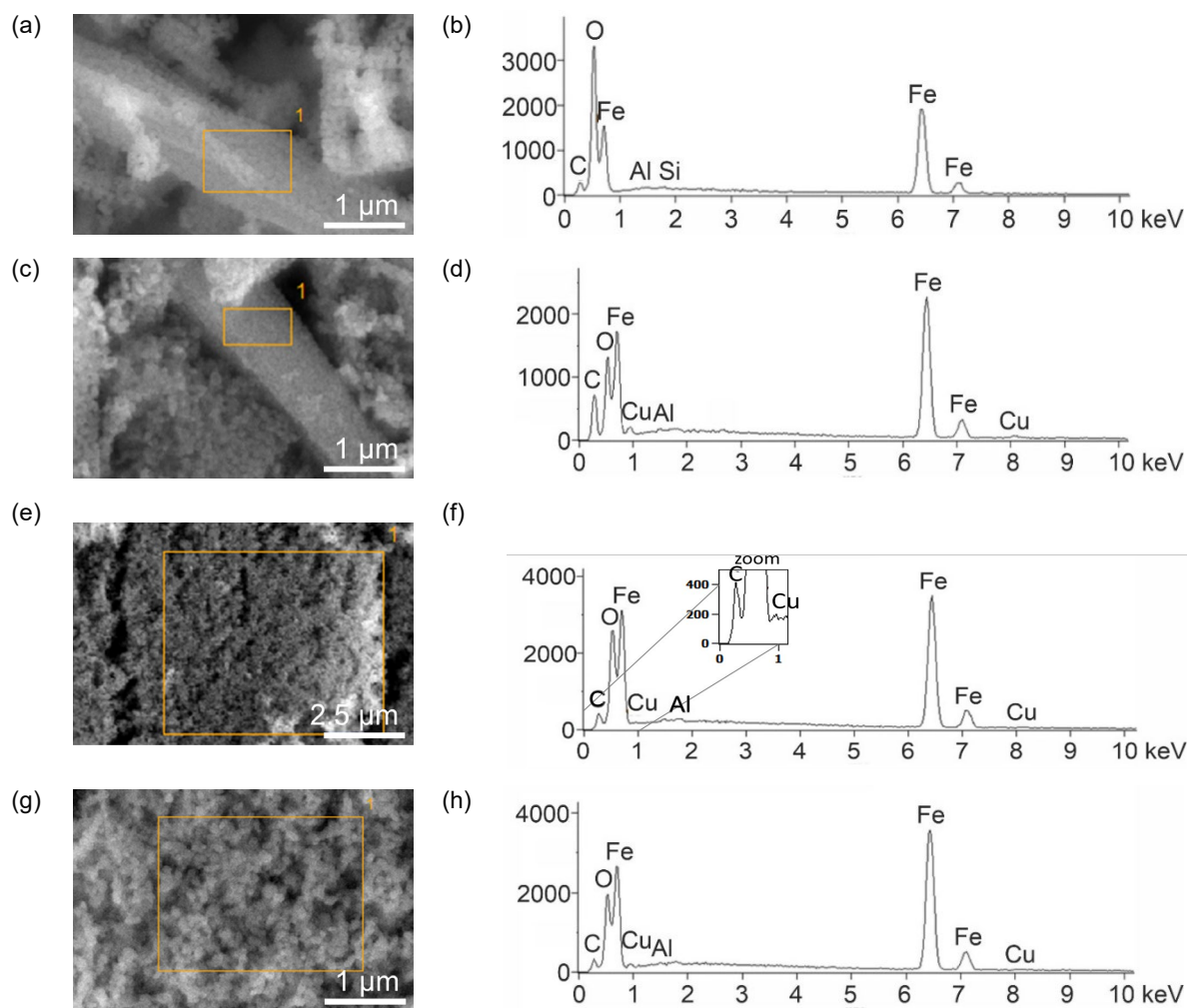


Figure S14. SEM images of the spent catalysts and EDX of the selected part of the image in highlighted rectangles with included particles, (a, b) spent FeO_x, (c, d) spent 1%-Cu/FeO_x, (e, f) spent 3%-Cu/FeO_x, (g, h) spent 5%-Cu/FeO_x.

STEM/HAADF images of spent FeO_x

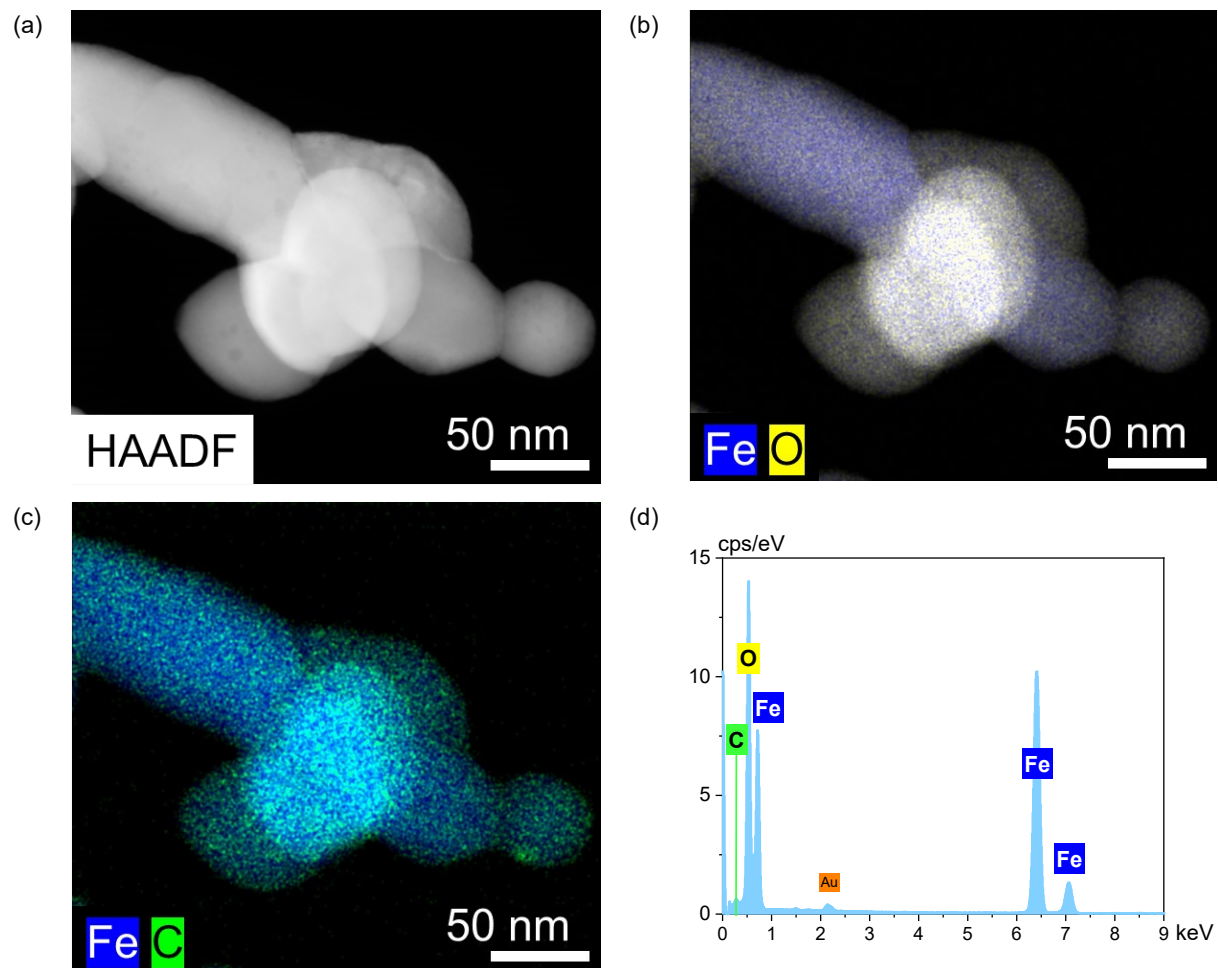


Figure S15. (a) STEM-HAADF of spent FeO_x, and (b-d) EDX elemental mapping of Fe, O, C and Cu.

STEM/HAADF images of spent 1%-Cu/FeO_x

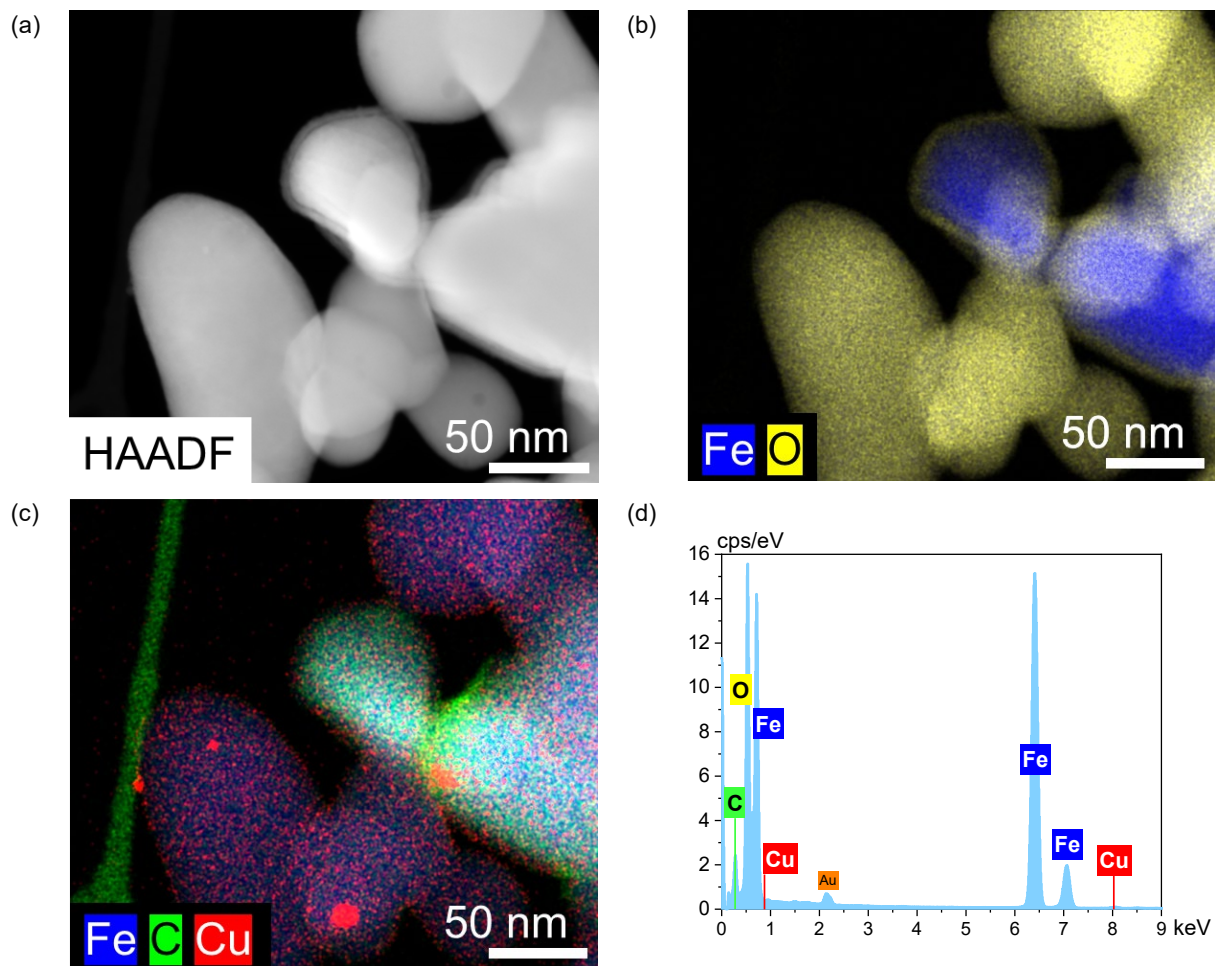


Figure S16. (a) STEM-HAADF of spent 1%-Cu/FeO_x, and (b-d) EDX elemental mapping of Fe, O, C and Cu.

STEM/HAADF images of spent 3%-Cu/FeO_x

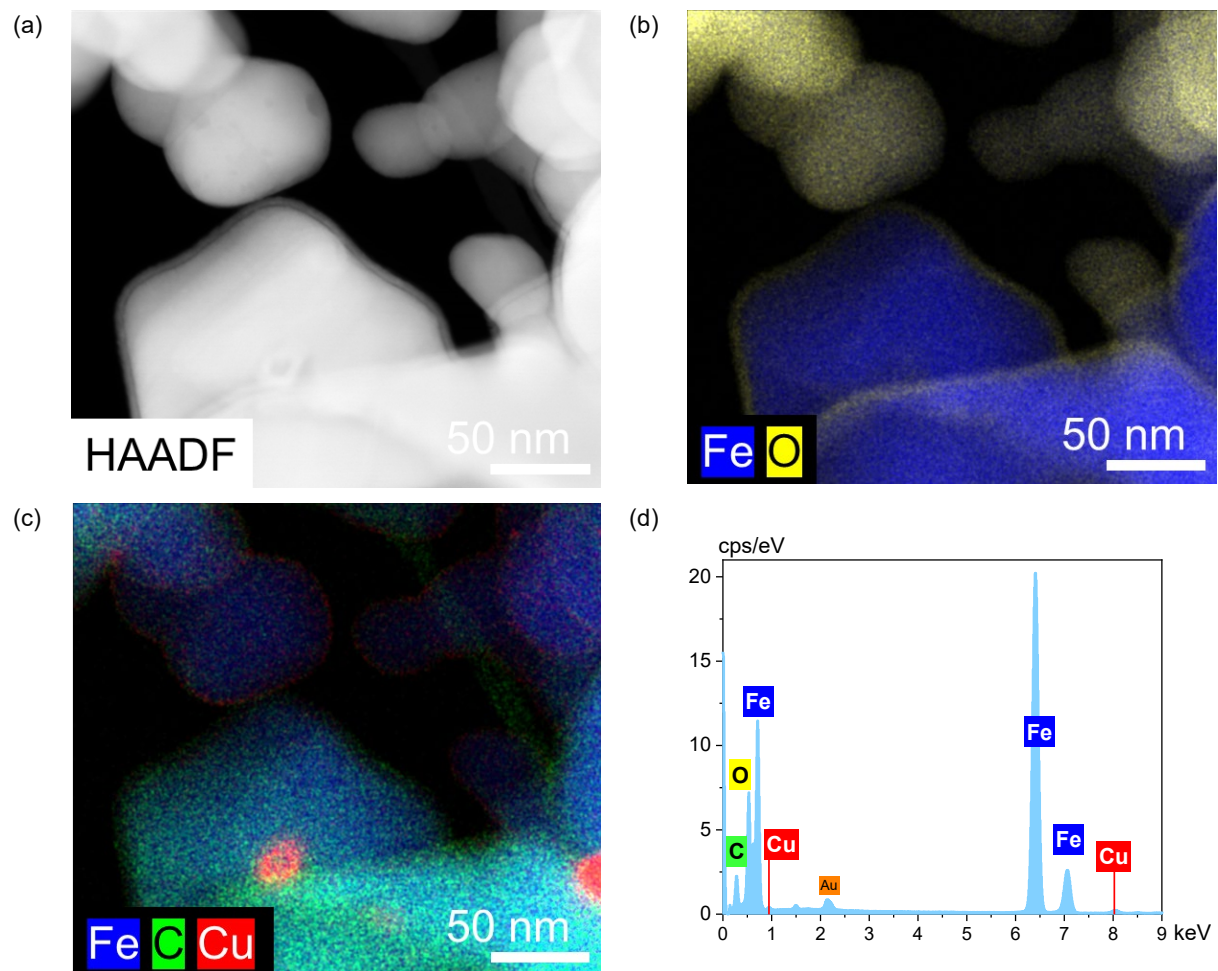


Figure S17. (a) STEM-HAADF of spent 3%-Cu/FeO_x, and (b-d) EDX elemental mapping of Fe, O, C and Cu.

XRD patterns of spent catalysts

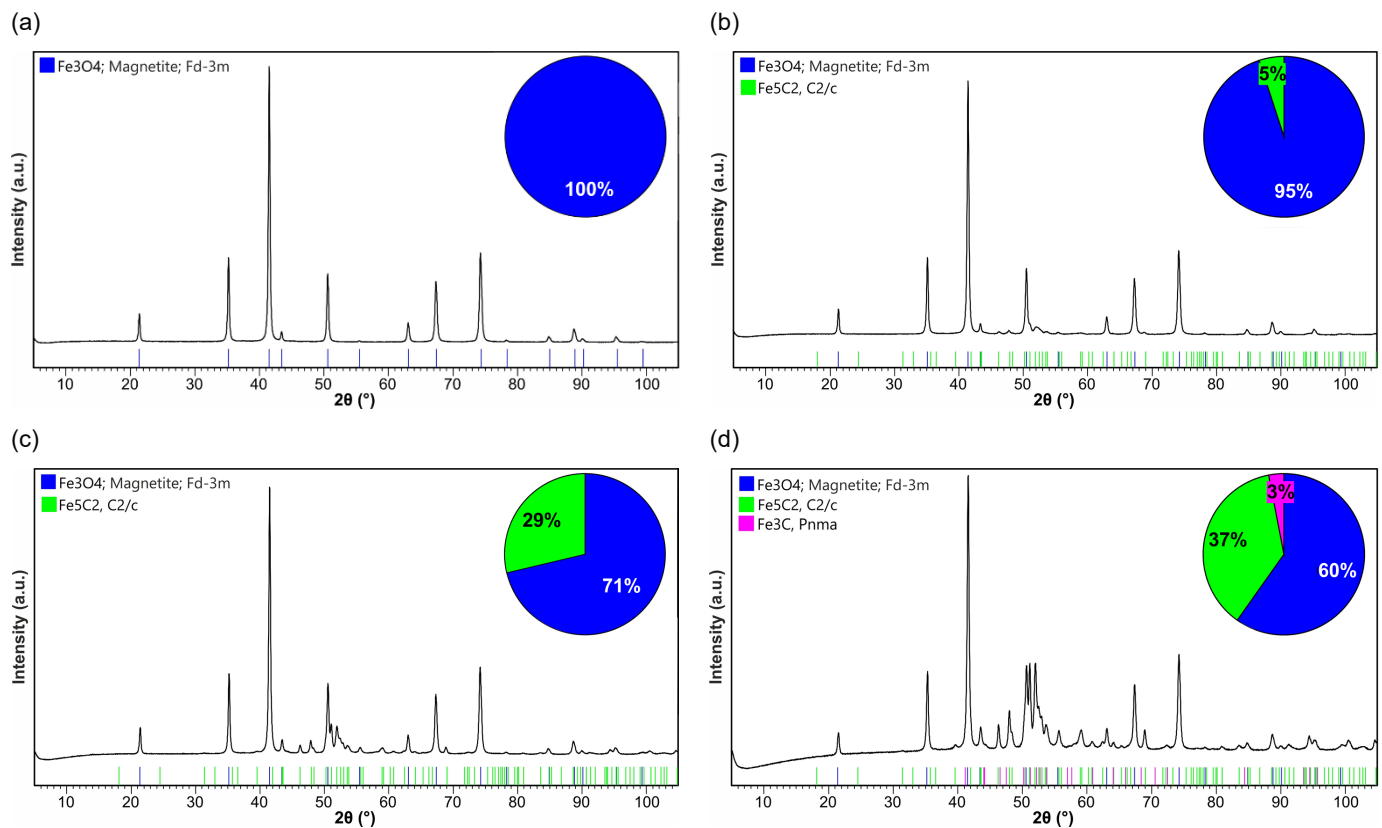


Figure S18. XRD patterns of spent (a) FeO_x , (b) $1\text{-Cu}/\text{FeO}_x$, (c) $3\text{-Cu}/\text{FeO}_x$ and (d) $5\text{-Cu}/\text{FeO}_x$.

Mean X-ray coherence length of spent catalysts

Table S4. Mean X-ray coherence length of spent catalysts obtained from XRD data using Rietveld refinement of analysis.

| Catalyst | Fe ₃ O ₄ [nm] | Fe ₅ C ₂ [nm] | Fe ₃ C [nm] |
|------------------------|--|--|---------------------------|
| FeO _x | 63.0 | 0.0 | 0.0 |
| 1%-Cu/FeO _x | 63.0 | 29.0 | 0.0 |
| 3%-Cu/FeO _x | 47.0 | 40.0 | 0.0 |
| 5%-Cu/FeO _x | 36.0 | 35.0 | 23.0 |

Adsorption/desorption isotherms of spent catalysts

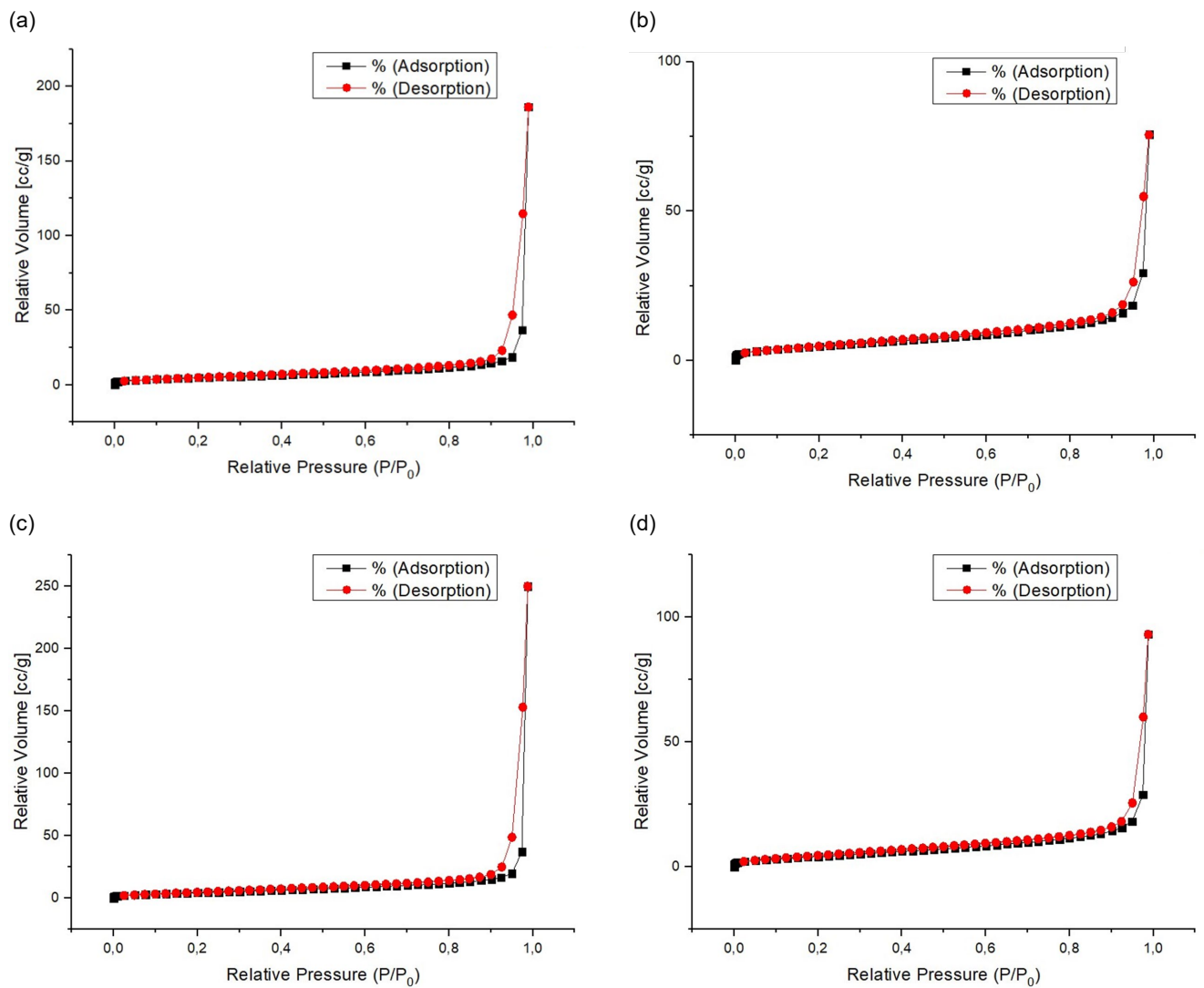


Figure S19. Adsorption and desorption isotherms of spent (a) FeO_x , (b) 1%-Cu/ FeO_x , (c) 3%-Cu/ FeO_x and (d) 5%-Cu/ FeO_x .

Comparison of the performance of the catalysts as the function of temperature during the second ramp

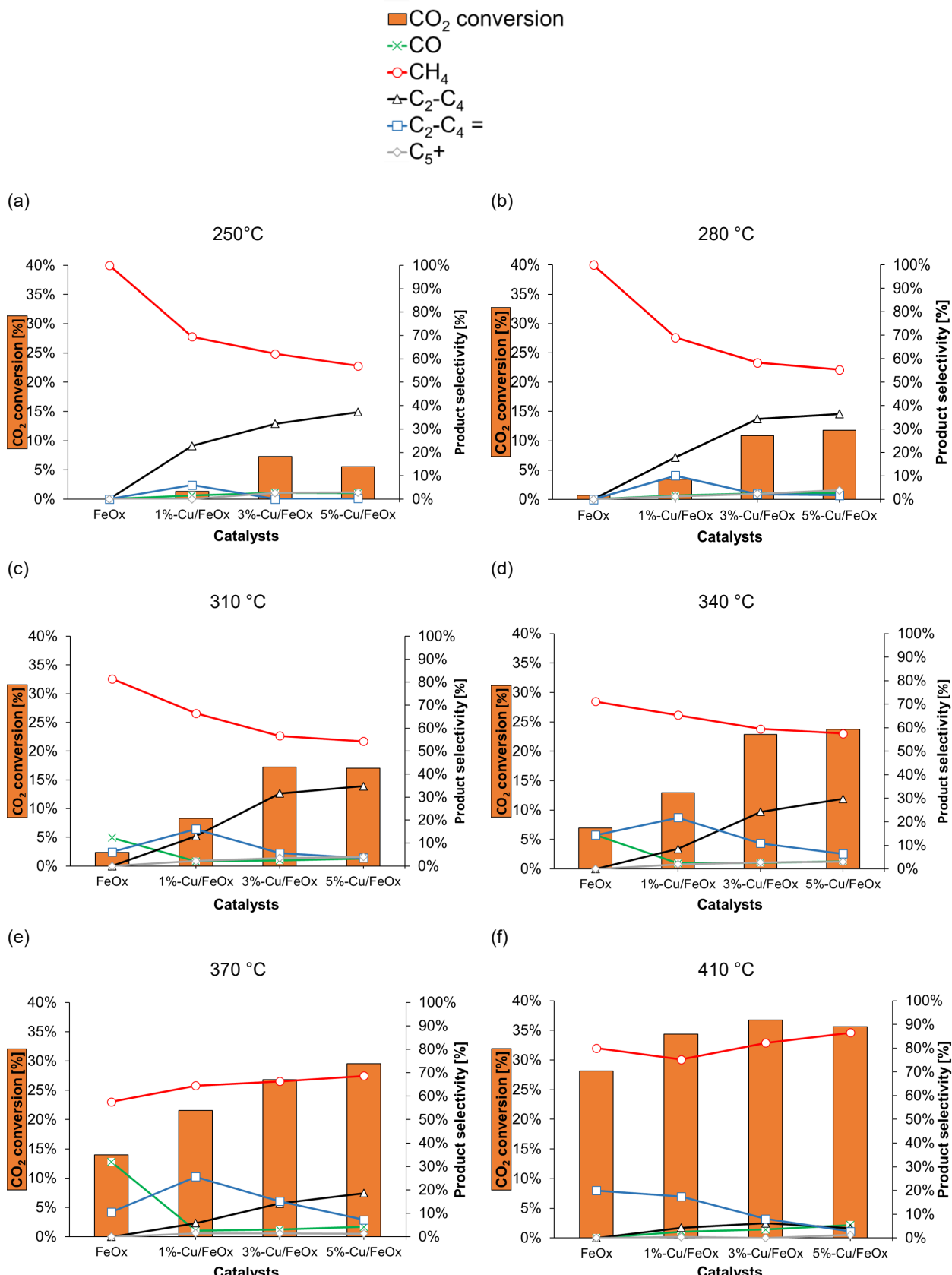


Figure S20. (a-f) CO₂ conversion and product selectivity of the studied catalysts as the function of temperature during the second temperature ramp.

CO₂ conversion over the course of six consecutive temperature ramps

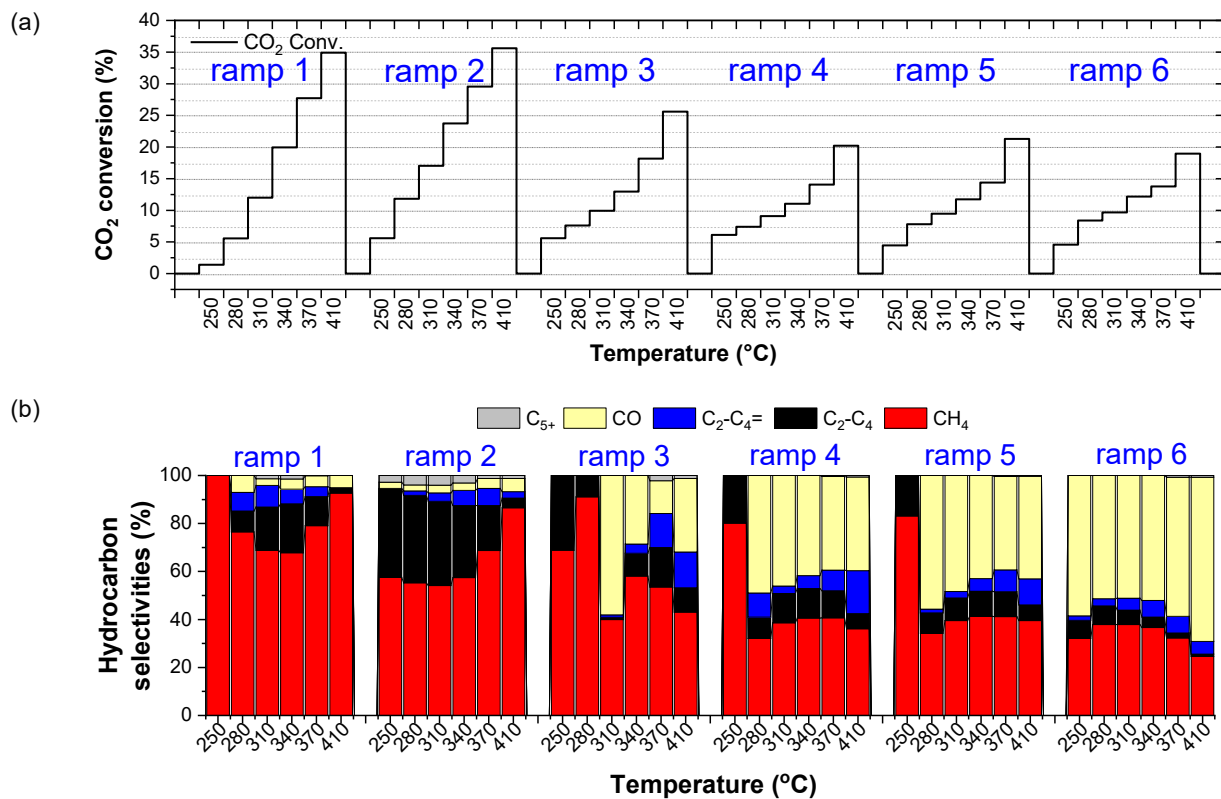


Figure S21. 5%-Cu/FeO_x. (a) CO₂ conversion throughout 6 consecutive temperature ramps. (b) Product selectivity throughout 6 consecutive temperature ramps. CO₂ 200 mg of catalyst and CO₂/H₂/He (1:5:4, total flow 25 ml/min).

Literature comparison of CO₂ hydrogenation by different iron-based catalysts

Table S5. Literature review of Fe-based catalysts for CO₂ hydrogenation

| Entry | Cat. | Temp. (°C) | Pretreatment | CO ₂ Conv. (%) | Selectivity (%) | | | | | Ref. |
|-------|---|------------|---|---------------------------|-----------------|------|----------------------------------|--------------------------------|------------------------------|------|
| | | | | | CH ₄ | CO | C ₂ -C ₄ = | C ₂ -C ₄ | C ₅ + and other s | |
| 1 | 1%-Cu/FeOx | 370 | None | 23.5 | 60.5 | 2.5 | 29 | 5.7 | 2.3 | * |
| 2 | 3%-Cu/FeO _x | 370 | None | 27.3 | 62.7 | 2.7 | 14.6 | 17.7 | 2.3 | * |
| 3 | 5%-Cu/FeO _x | 370 | None | 27.8 | 78.3 | 4.4 | 4.5 | 12.3 | 0.4 | * |
| 4 | Fe-Mn-K | 300 | H ₂ :CO=2:1, 320°C, 24h | 38.2 | 10.4 | 5.6 | 25.2 | 2 | 61.9 | [1] |
| 5 | Fe-Co/Al ₂ O ₃ -K | 300 | H ₂ , 400°C, 2h | 36 | 16 | 13 | - | 71 | - | [2] |
| 6 | Fe/Co-Y | 300 | H ₂ , 380°C, 8h | 29.6 | 14 | 21 | - | 30 | 55 | [3] |
| 7 | Na/FeOx | 320 | H ₂ , 350°C, 12h | 36 | 8 | 10 | 64 | 18 | - | [4] |
| 8 | Ru-FeOx/Al ₂ O ₃ | 300 | H ₂ , 300°C | 18 | 55 | - | - | 45 | - | [5] |
| 9 | Fe-Ru-K | 300 | H ₂ , 450°C, 5h | 47 | 16.4 | 3.1 | 19.7 | 7.4 | 53 | [6] |
| 10 | Fe-K/alumina | 300 | H ₂ , 450°C, 13h | 31.3 | 11 | 7 | - | 36 | 46 | [7] |
| 11 | Fe/CNT | 350 | H ₂ , 400°C, 2h | 20 | 36 | 22 | - | 33 | 9 | [8] |
| 12 | Cu/Fe ₂ O ₃ | 300 | H ₂ , 400°C, 2h | 17 | 2-3 | 31 | - | 32 | 65 | [9] |
| 13 | Na-Fe ₃ O ₄ /HMCM | 320 | H ₂ , 350°C, 8h | 26 | 8 | 17 | - | 26 | 57 | [10] |
| 14 | ZnFe ₂ O ₄ | 340 | H ₂ , 400°C, 2h | 28 | 44 | 22 | - | 34 | - | [11] |
| 15 | Fe-Ru-Mn-K/Al ₂ O ₃ | 300 | 10% H ₂ , 500°C, 2h | 30 | 19 | 18 | - | 39 | 25 | [12] |
| 16 | Co-Fe | 270 | CO, 250°C, 20h | 23 | 31 | 53 | - | 12 | - | [13] |
| 17 | Mn-Na-Fe | 320 | H ₂ , 350°C, 12h | 38.6 | 11.8 | 11.8 | 30.2 | 4 | 42.1 | [14] |
| 18 | Fe-Ce | 300 | 33% H ₂ , 400°C, 16h; 33% CO, 400°C, 16h | 25 | 38 | 19 | - | 38 | 4 | [15] |
| 19 | Na-Fe ₃ O ₄ | 320 | H ₂ , 350°C, 12h | 40.5 | 15.8 | 13.5 | 46.6 | 7.5 | 30.1 | [16] |
| 20 | Mn/Fe ₃ O ₄ -EDA | 320 | None | 20 | 40 | 41 | 1 | 36 | 23 | [17] |
| 21 | K-FeC/ZrO ₂ | 220 | H ₂ , 400°C, 4h | 40 | 13 | 32 | 25 | - | 30 | [18] |
| 22 | Fe-Cu-K-Al | 300 | CO, 350°C, 4h | 41 | 15.6 | 2.5 | - | 38 | 44 | [19] |
| 23 | Fe-Cu-K | 300 | H ₂ , 400°C, 2h | 29.7 | 7 | 17 | 22 | - | 54 | [20] |
| 24 | Na-CoFe ₃ O ₄ | 320 | H ₂ , 400°C, 3h | 34 | 15 | - | 39 | 6 | 40 | [21] |
| 25 | Fe ₂ O ₃ | 300 | 50% H ₂ , 500°C, 2h | 23 | 14 | n.a | - | - | 65 | [22] |
| 26 | K-Fe ₂ O ₃ | 270 | H ₂ :CO=1:1, 350°C, 1h | 36 | 20 | 13 | 35 | 8 | 24 | [23] |
| 27 | Mn-FeO | 340 | H ₂ , 400°C, 5h | 30 | 40 | 7 | - | 52 | n.a | [24] |

* This work.

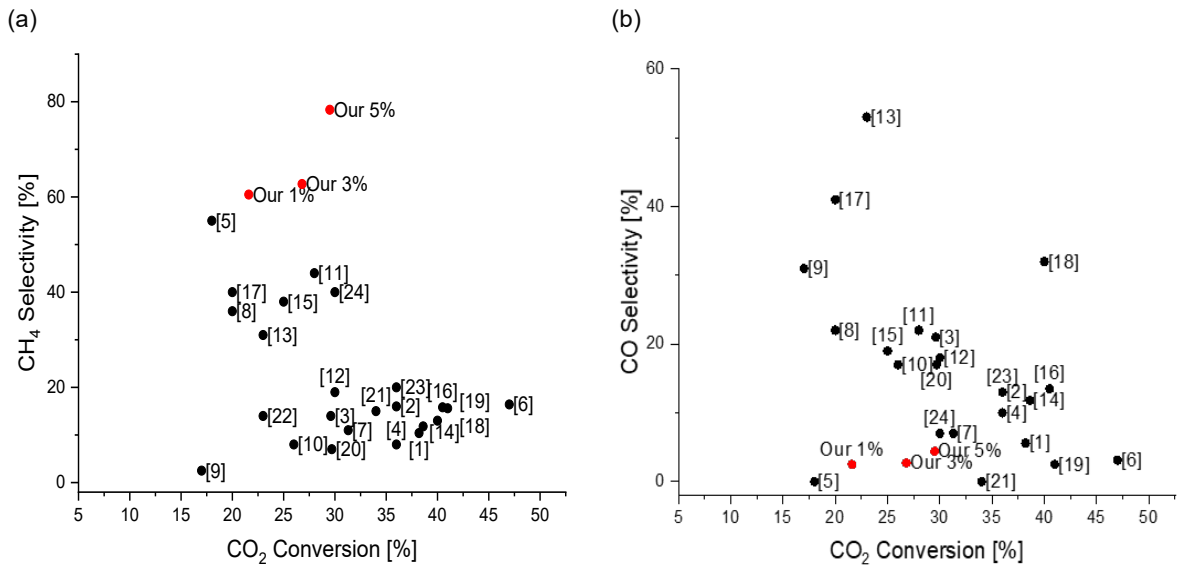


Figure S22. (a) CH₄ selectivity plotted against CO₂ conversion and (b) CO selectivity plotted against CO₂ conversion for catalysts from literature review (**Table S5**) including reference numbers. Our catalysts are red points.

References

- Yao, B.; Xiao, T.; Makgae, O.A.; Jie, X.; Gonzalez-Cortes, S.; Guan, S.; Kirkland, A.I.; Dilworth, J.R.; Al-Megren, H.A.; Alshihri, S.M., et al. Transforming Carbon Dioxide into Jet Fuel Using an Organic Combustion-Synthesized Fe-Mn-K Catalyst. *Nat Commun* **2020**, 11 (1), 6395.
- Satthawong, R.; Koizumi, N.; Song, C.; Prasassarakich, P. Bimetallic Fe–Co Catalysts for Co₂ Hydrogenation to Higher Hydrocarbons. *J. CO₂ Util.* **2013**, 3-4, 102-106.
- Guo, L.; Cui, Y.; Li, H.; Fang, Y.; Prasert, R.; Wu, J.; Yang, G.; Yoneyama, Y.; Tsubaki, N. Selective Formation of Linear-Alpha Olefins (Laos) by Co₂ Hydrogenation over Bimetallic Fe/Co-Y Catalyst. *Catal Commun* **2019**, 130, 105759.
- Liang, B.; Duan, H.; Sun, T.; Ma, J.; Liu, X.; Xu, J.; Su, X.; Huang, Y.; Zhang, T. Effect of Na Promoter on Fe-Based Catalyst for Co₂ Hydrogenation to Alkenes. *ACS Sustain. Chem. Eng* **2019**, 7 (1), 925-932.
- Aitbekova, A.; Goodman, E.D.; Wu, L.; Boubnov, A.; Hoffman, A.S.; Genc, A.; Cheng, H.; Casalena, L.; Bare, S.R.; Cargnello, M. Engineering of Ruthenium–Iron Oxide Colloidal Heterostructures: Improved Yields in Co₂ Hydrogenation to Hydrocarbons. *Angew. Chem. Int. Ed.* **2019**, 58 (48), 17451-17457.
- Jiang, F.; Liu, B.; Geng, S.; Xu, Y.; Liu, X. Hydrogenation of Co₂ into Hydrocarbons: Enhanced Catalytic Activity over Fe-Based Fischer–Tropsch Catalysts. *Catal. Sci. Technol.* **2018**, 8 (16), 4097-4107.
- Hwang, J.S.; Jun, K.-W.; Lee, K.-W. Deactivation and Regeneration of Fe-K/Alumina Catalyst in Co₂ Hydrogenation. *APPL CATAL A-GEN* **2001**, 208 (1), 217-222.
- Chernyak, S.A.; Ivanov, A.S.; Stolbov, D.N.; Maksimov, S.V.; Maslakov, K.I.; Chernavskii, P.A.; Pokusaeva, Y.A.; Koklin, A.E.; Bogdan, V.I.; Savilov, S.V. Sintered Fe/Cnt Framework Catalysts for Co₂ Hydrogenation into Hydrocarbons. *Carbon* **2020**.
- Choi, Y.H.; Jang, Y.J.; Park, H.; Kim, W.Y.; Lee, Y.H.; Choi, S.H.; Lee, J.S. Carbon Dioxide Fischer-Tropsch Synthesis: A New Path to Carbon-Neutral Fuels. *Appl Catal B* **2017**, 202, 605-610.
- Wei, J.; Yao, R.; Ge, Q.; Wen, Z.; Ji, X.; Fang, C.; Zhang, J.; Xu, H.; Sun, J. Catalytic Hydrogenation of Co₂ to Isoparaffins over Fe-Based Multifunctional Catalysts. *ACS Catal.* **2018**, 8 (11), 9958-9967.
- Choi, Y.H.; Ra, E.C.; Kim, E.H.; Kim, K.Y.; Jang, Y.J.; Kang, K.-N.; Choi, S.H.; Jang, J.-H.; Lee, J.S. Sodium-Containing Spinel Zinc Ferrite as a Catalyst Precursor for the Selective Synthesis of Liquid Hydrocarbon Fuels. *ChemSusChem* **2017**, 10 (23), 4764-4770.
- Rodemerck, U.; Holeňa, M.; Wagner, E.; Smejkal, Q.; Barkschat, A.; Baerns, M. Catalyst Development for Co₂ Hydrogenation to Fuels. *ChemCatChem* **2013**, 5 (7), 1948-1955.
- Gnanamani, M.K.; Jacobs, G.; Hamdeh, H.H.; Shafer, W.D.; Liu, F.; Hopps, S.D.; Thomas, G.A.; Davis, B.H. Hydrogenation of Carbon Dioxide over Co–Fe Bimetallic Catalysts. *ACS Catal.* **2016**, 6 (2), 913-927.
- Liang, B.; Sun, T.; Ma, J.; Duan, H.; Li, L.; Yang, X.; Zhang, Y.; Su, X.; Huang, Y.; Zhang, T. Mn Decorated Na/Fe Catalysts for Co₂ Hydrogenation to Light Olefins. *Catal. Sci. Technol.* **2019**, 9 (2), 456-464.
- Pérez-Alonso, F.J.; Ojeda, M.; Herranz, T.; Rojas, S.; González-Carballo, J.M.; Terreros, P.; Fierro, J.L.G. Carbon Dioxide Hydrogenation over Fe–Ce Catalysts. *Catal Commun* **2008**, 9 (9), 1945-1948.
- Wei, J.; Sun, J.; Wen, Z.; Fang, C.; Ge, Q.; Xu, H. New Insights into the Effect of Sodium on Fe₃O₄- Based Nanocatalysts for Co₂ Hydrogenation to Light Olefins. *Catal. Sci. Technol.* **2016**, 6 (13), 4786-4793.
- Liu, B.; Geng, S.; Zheng, J.; Jia, X.; Jiang, F.; Liu, X. Unravelling the New Roles of Na and Mn Promoter in Co₂ Hydrogenation over Fe₃O₄-Based Catalysts for Enhanced Selectivity to Light A-Olefins. *ChemCatChem* **2018**, 10 (20), 4718-4732.
- Zhu, J.; Zhang, G.; Li, W.; Zhang, X.; Ding, F.; Song, C.; Guo, X. Deconvolution of the Particle Size Effect on Co₂ Hydrogenation over Iron-Based Catalysts. *ACS Catalysis* **2020**, 10 (13), 7424-7433.
- Hong, J.-S.; Hwang, J.S.; Jun, K.-W.; Sur, J.C.; Lee, K.-W. Deactivation Study on a Coprecipitated Fe–Cu–K–Al Catalyst in Co₂ Hydrogenation. *APPL CATAL A-GEN* **2001**, 218 (1), 53-59.
- Wang, W.; Jiang, X.; Wang, X.; Song, C. Fe–Cu Bimetallic Catalysts for Selective Co₂ Hydrogenation to Olefin-Rich C₂⁺ Hydrocarbons. *Ind. Eng. Chem. Res.* **2018**, 57 (13), 4535-4542.
- Kim, K.Y.; Lee, H.; Noh, W.Y.; Shin, J.; Han, S.J.; Kim, S.K.; An, K.; Lee, J.S. Cobalt Ferrite Nanoparticles to Form a Catalytic Co–Fe Alloy Carbide Phase for Selective Co₂ Hydrogenation to Light Olefins. *ACS Catal.* **2020**, 10 (15), 8660-8671.
- Albrecht, M.; Rodemerck, U.; Schneider, M.; Bröring, M.; Baabe, D.; Kondratenko, E.V. Unexpectedly Efficient Co₂ Hydrogenation to Higher Hydrocarbons over Non-Doped Fe₂O₃. *Appl Catal B* **2017**, 204, 119-126.
- Visconti, C.G.; Martinelli, M.; Falbo, L.; Infantes-Molina, A.; Lietti, L.; Forzatti, P.; Iaquaniello, G.; Palo, E.; Picutti, B.; Brignoli, F. Co₂ Hydrogenation to Lower Olefins on a High Surface Area K-Promoted Bulk Fe-Catalyst. *Appl Catal B* **2017**, 200, 530-542.

24. Al-Dossary, M.; Ismail, A.A.; Fierro, J.L.G.; Bouzid, H.; Al-Sayari, S.A. Effect of Mn Loading onto Mnfeo Nanocomposites for the Co₂ Hydrogenation Reaction. *Appl Catal B* **2015**, 165, 651-660.